Zakariae Jebroni[1,*], Hajar Chadli[2], Elhassane Chadli[2], Belkassem Tidhaf[1]

J. Electrical Systems 13-4 (2017): 806-823

Journal of Electrical Systems

Remote calibration system of a smart electrical energy meter

The need to control the power grid in real time has opened a new field of research, today researchers are trying to design electrical meters that are completely remote controlled, to create an advanced metering infrastructure. One of the most important processes in the field of measurement is the calibration of measuring instruments. The calibration process of the electrical meters was performed at laboratories. However, the new directives, now, require a regular test of accuracy. Nevertheless, moving each time on site to check the accuracy of a meter can be annoying. To solve this problem our contribution is to propose a new structure of a smart meter that integrates a calibration card, so that, this process is carried out remotely. To be able to calibrate the meter or test its accuracy, we have included an AC-AC converter powered by the electrical grid and that provides a stable voltage independent of the electrical grid in term of frequency and amplitude. The output voltage of the converter is used as the reference signal during calibration or accuracy testing. In this paper, we will present the structure of the calibration card, the study and dimensioning of the converter, as well as the control technique used to eliminate variations of the input voltage. At the end, we will present the results of simulations and experiments.

Keywords: Remote calibration; calibration on site; AC-AC converter; unipolar PWM technique; Smart meter structure.

Article history: Received 5 July 2017, Accepted 10 November 2017

1. Introduction

Electrical energy meters are measurement instruments that are widely used, since at present, almost every inhabitant in the world uses electrical energy. The utility of these meters is to measure the electrical energy consumed by the customer. Thus, the provider of electricity uses this information to bill the customer.

The first electrical meter used is the electromechanical meter; it is not communicating and it could measure via the induction effect and display only one type of energy e.g. the active energy. As the number of customers grew, the electricity providers found difficulties to record the consumption information manually and monthly. Therefore, it has appeared the Automatic Meters Reading (AMR)[1]–[6], where the process of data reading has been automated by programming the meter to send the data periodically. After the innovation of the AMRs, other problems appeared which are related to the distributed networks, the management and the diagnostics. Therefore, the suppliers noted that they had to manage the electricity network in real time. Currently, the researchers work on the automation, the real time management and remote control of the electrical network infrastructure, what is called Advanced Metering

* Corresponding author: Zakariae Jebroni, E-mail: zakariae.jebroni@gmail.com.

1 Laboratory of Embedded Electronic Systems and Renewable Energy, University Mohammed First Oujda, Morocco

2 Laboratory Electronics and Systems, University Mohammed First Oujda, Morocco

Infrastructure (AMI) [7]–[15]. In these works we focus on two essentials points: the smart meter and the control central. To control the electrical network remotely, we must first have accurate information of the consumption and the production of the electrical energy. Therefore, the meter must send accurate information. However, these meters are manufactured by electronics components and integrated circuits that can cause errors during measurement. For this reason, the first step after manufacturing or maintaining the meter is to eliminate the error of the measure by the calibration process. In this step, the meter is powered by a known power source used as a reference, and based on the measurement and reference values, the error (or errors) is calculated and then eliminated either analogically or by programming the integrated measurement circuit.

The electrical energy meters have been calibrated at laboratories. However, the problem was that if a meter would require an accuracy check or if it did not work, it would have to be brought back to the laboratory. In addition, the directives for measurement instruments are becoming more and more stringent, for example in Europe, they require that the measurement instruments should be tested periodically and on site [16]. This gave birth to the idea of on-site calibration [16]–[25]. These researches propose external equipment used to test the accuracy of electrical energy meters. Since these equipments are independent of the meter (not of the same manufacturer), if this latter requires correction of errors, it must be returned to the laboratory. Moreover, to cover an enormous number of customers (5392479 in Morocco [26]) and test their meters periodically, it is necessary to prepare a hundred teams dedicated to this effect.

We can draw two major problematic:

- These calibration equipments can not interact and correct measurement errors if there is.
- We have to move on site to perform this operation, but it is difficult to manage a huge number of customers.

As a result, our contribution is to integrate the calibration circuit into the electricity meter instead of using external equipment. And since the electric meter is remotely controlled (the principle of advanced measurement infrastructure), this will allow the accuracy test to be carried out, so that measurement errors can be corrected without moving a team and without having made the electricity meter in the laboratory. When we were designing the calibration card, we noticed that we should add a power source used as a reference, because when we want to test the accuracy or perform the calibration on site, we cannot know how much is exactly the voltage of the electrical grid, because this latter can vary [27]. Then we designed an AC-AC converter included in the calibration card. This converter is powered by the electrical grid voltage, and provides a stable voltage at the output. Furthermore, we used a known load to fix the current. These two electrical quantities (current and voltage) act as references of our measurement system during the calibration procedure.

In this paper, we will first describe the operation of the calibration card and the remote calibration system. Then we will present the study and dimensioning of the AC-AC converter. Then we will present simulations results and experiments results. Finally, we will end with a conclusion.

2. Overview of the new remote calibration system

In our research work we realize a Smart Electrical Energy Meter (SEEM). This measurement instrument is intended for the low-voltage single-phase customers. Currently the researchers develop this kind of instrument to be totally remote controlled [28], [29], because of the increasing of customers and the need of the real-time monitoring. During the study, we deduced that the calibration step is one of important steps either during manufacturing or during maintenance. Moreover, this step should be performed on site and remotely for these reasons:

- The calibration on site takes into account the electromagnetic perturbations.
- The accuracy check of the meters will be performed without having moving a team.
- During maintenance, if the meter was broken, we do not need to take it to the laboratory, for the calibration.

When we want to perform the meter calibration, we need, at that moment, to know how much is the value of the electrical measured quantities (current and voltage). However, the voltage of the electrical grid can vary. For example in Morocco, the voltage can vary between 80% and 115% of the nominal value [27]. Therefore, we cannot use this power source as reference. Furthermore with a basic structure of a digital meter (figure 1(a)) we cannot perform the meter calibration because this instrument is connected directly, trough sensors, to the electrical grid. So, we developed a new meter structure and we added a calibration card into the meter to perform the calibration process on site and remotely (figure 1(b)).

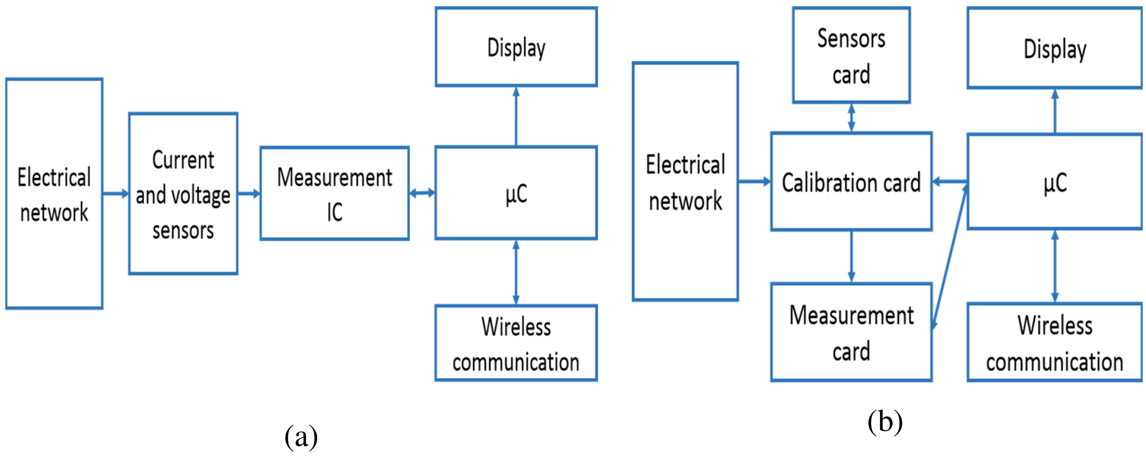

Figure 1: (a) Structure of basic digital meter. (b) Structure of proposed digital meter.

The block diagram of the proposed electrical meter is shown in figure 2. The electrical flow passes first through the calibration card. This flow is then passed through current and voltage sensors. These sensors provide at the output attenuated signals that represent current and voltage. Then this analog signals are converted into digital signals and filtered through a special measurement circuit.

The communication between the measurement circuit and the processing card ,built around a microcontroller, is provided by connectors. At the microcontroller being the central unit of the measurement system, the data from the measurement circuit are processed in order to display them and send them via a wireless transmission.

It should be noted that the circuit is designed to control remotely the calibration card. This is done by sending instructions to the electrical meter, which are captured by the communication module and executed by the microcontroller. This one controls the relays of the calibration card.

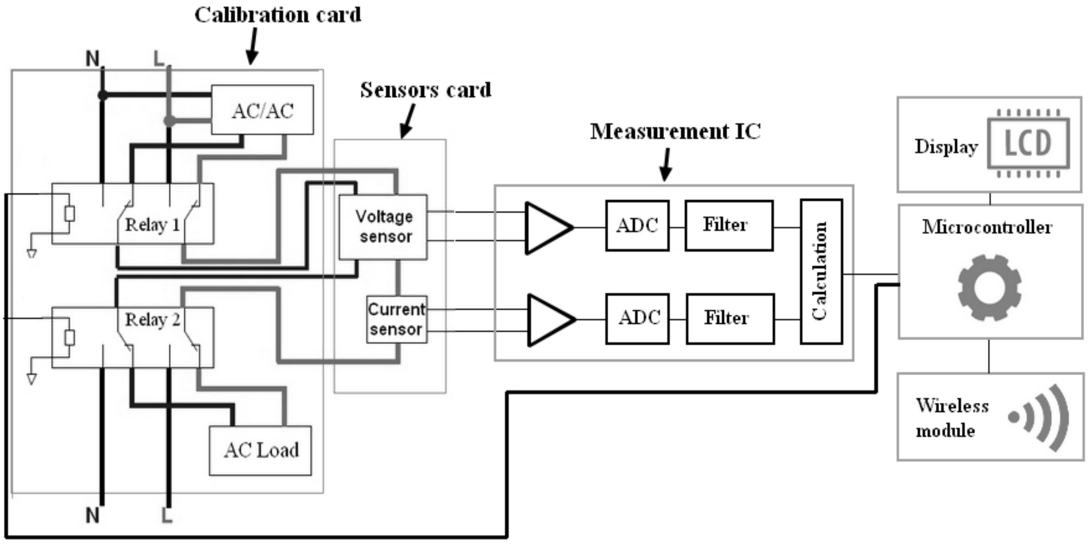

Figure 2: Block diagram of the electrical meter.

The block diagram of the calibration card, shown in figure 3, contains several blocks. The most important block that should be studied is the AC-AC converter, and that we will present his design in following section.

We distinguish two modes of use of the electrical meter, the count mode and the calibration mode. In the first mode (figure 4(a)) relay 1, which selects the source of energy, selects the electrical grid as source, while relay 2 redirects the energy to the home. In the second mode (figure 4(b)), the relay 1 selects the AC-AC converter as a source of energy while the relay 2 redirects this energy to the AC load.

The role of the converter is to provide a stable voltage at its output whatever the variation of the input voltage, in order to be able to calculate the measurement errors with reference to this voltage.

The role of the AC load is to set the current value to a specific value in order to use it as a reference. In addition, it is necessary to create a phase shift between the current and the voltage to be able to compensate that added by the measuring components [24], [30].

3. Design of the AC-AC converter and the AC load

The converter will play the role of a power source that provide a stable voltage at the output. Furthermore, it supplies an AC load. Therefore, the converter will stabilize the voltage, while the load will fix the current. To design this converter we posed the following specifications:

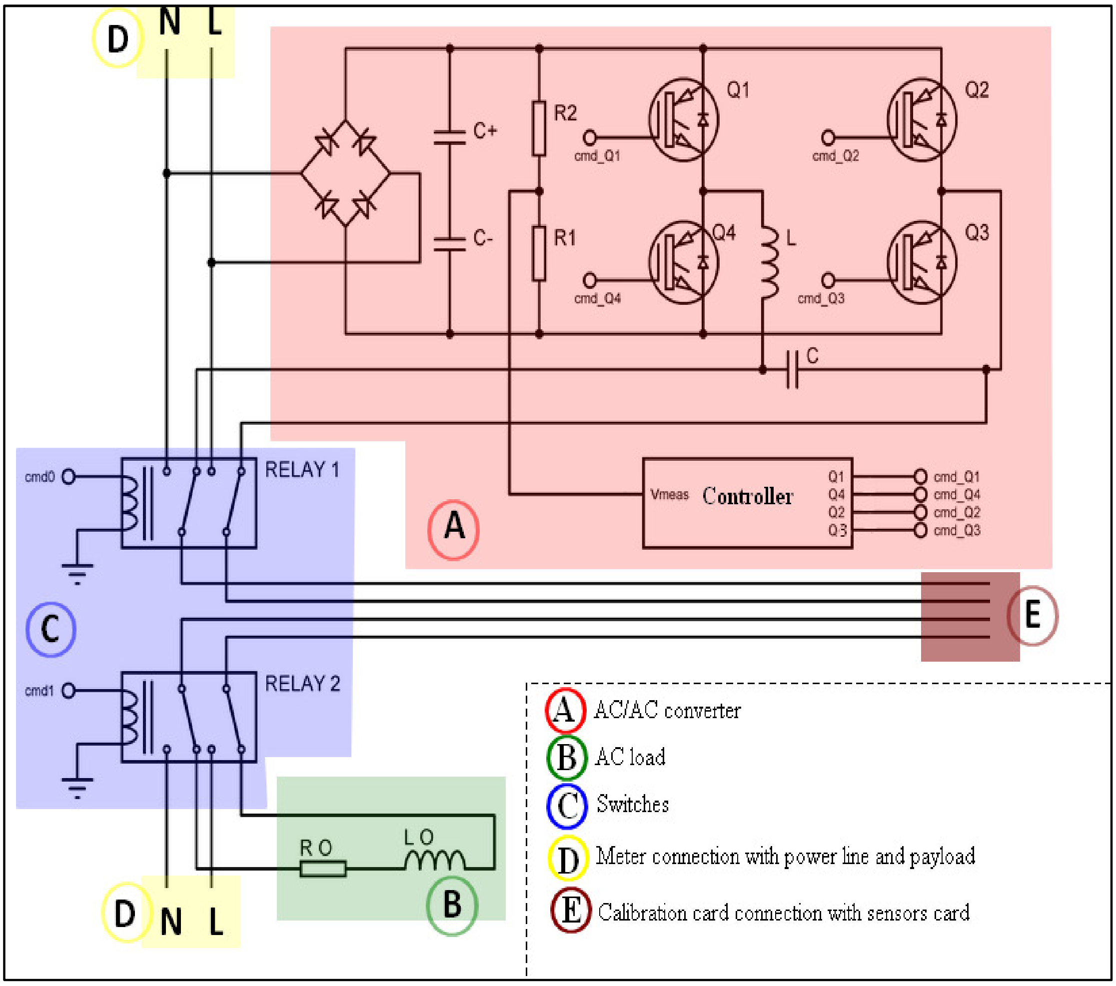

Figure 3: Block diagram of the calibration card.

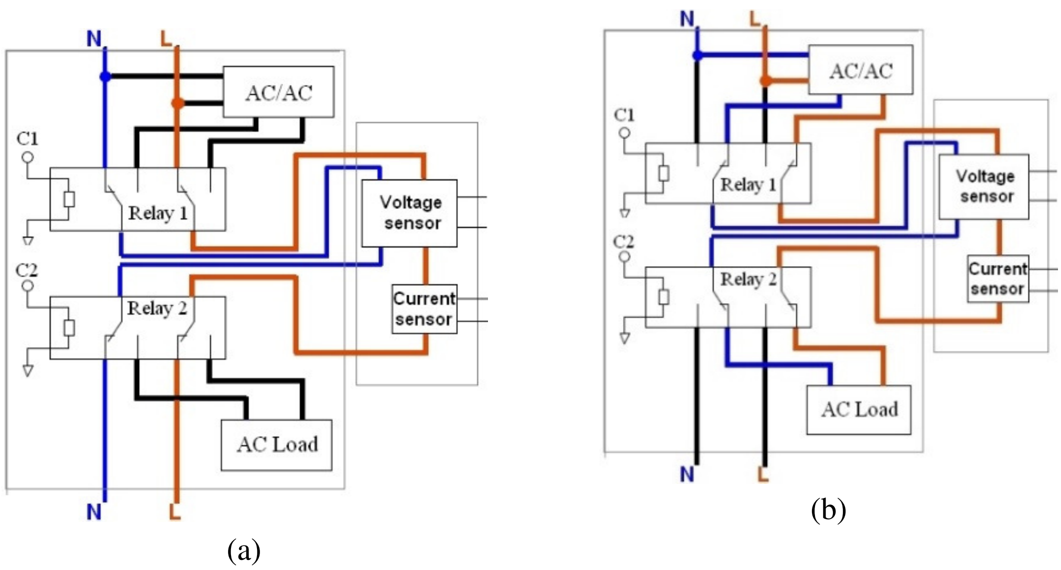

Figure 4: (a) Calibration card used in count mode. (b) Calibration card used in calibration mode.

- The converter is supplied by the electrical grid. So, we must compensate the input voltage variations.
- The converter provide a power equals 600VA, with an AC output voltage equals $120V_{RMS}$ and an AC output current equals $5A_{RMS}$
- The power factor should equals 0.5 to be able to compensate the phase shift added by the measurement system.
- The calibration process is independent of the electrical grid at the time of measurement of the references, so we do not need synchronization between the electrical grid and the AC-AC converter.

It should be noted that the choose of these values is not arbitrary. We respected the specifications of the measurement integrated circuit "CS5490" [30], as well as the calculation is fully detailed in the paper [24].

3.1. Design of the power part of the converter

The converter designed is an indirect, single-phase AC-AC converter. The AC input voltage passes by a rectifier bridge, then we used a Voltage Source Inverter (VSI) that provide an AC voltage at the output.

Figure 5 illustrates the scheme of the converter. We have chosen this simple structure, because the converter will be integrated into the meter. Thus, the calibration card should be small, then, it should contain the minimum of components.

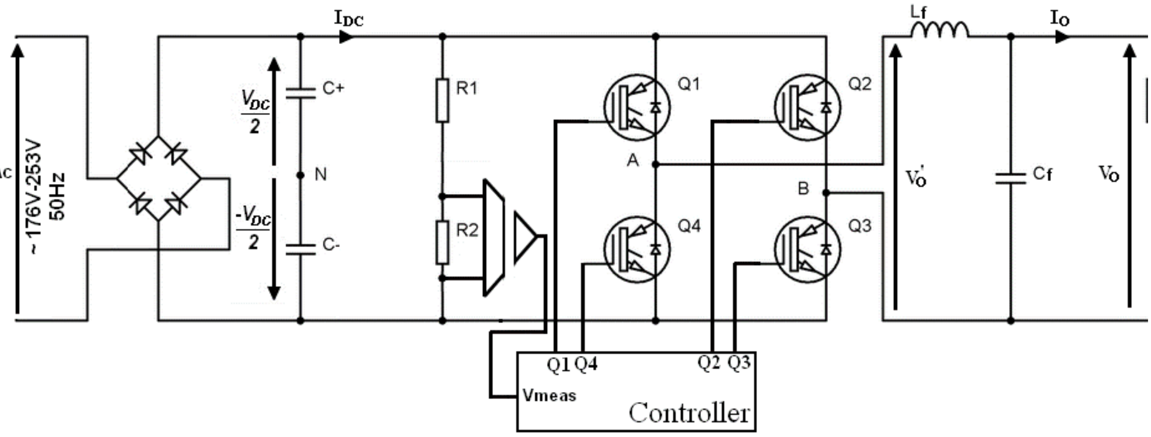

Figure 5: Power circuit of the AC-AC converter.

In this type of applications, the choose of the components values is very important. We must sizing the diodes bridge of the rectifier, the capacitor filter, the switches, the LC filter and the AC load.

3.1.1. Rectifier

For the diodes, we must take in consideration the forward current and the maximum repetitive reverse voltage. The forward current who crosses the diodes is the same DC link current that supplies the inverter. This current is calculated by:

$$I_{DC} = \frac{V_O . I_O}{V_{DC}} \cos\varphi \tag{1}$$

Where Vo is the AC output voltage of the converter, Io is the AC output current of the converter, V_{DC} is the DC link voltage and $\cos\varphi$ is the power factor.

Regarding the filter capacitor, we calculate the value of capacitors with:

$$C_{TOT} = \frac{I_{DC}}{2. f. \Delta V_{DC}} \tag{2}$$

Where f is the frequency of the AC input voltage and ΔV_{DC} is the AC input voltage ripple. We note that we used two capacitors to create a neutral point and we have: $C+ = C- = 2C_{TOT}$.

3.1.2. Switches

We used in our application the IGBT switches IHW40N60R. These switches support a high switching frequency. Moreover, they can reach a collector-emitter voltage equals 600V and a collector current equals 40A.

3.1.3. AC load

The role of the AC load is to consume a known current that will be used as reference. Furthermore, it must create a 60° phase shift. This phase shift is used to compensate the phase added by the measurement system. We used in the application an inductive load. To calculate the values of the load elements we use these formulas:

$$\sqrt{{R_O}^2 + (L_O\omega)^2} = {}^{V_O}/_{I_O} \tag{3}$$

$${}^{L_O\omega}/_{R_O} = \tan(60\,°) \tag{4}$$

3.1.4. Filter

The VSI generate a voltage that contains a sum of harmonics. To have a sinusoidal waveform at the output of the converter, we must eliminate all harmonics and leave only the fundamental component. To do that, we should use a low pass filter. Generally, a LC filter is used in this type of applications [31]–[34].

To sizing well the converter, we must take into account the increasing and decreasing of the input voltage, the maximum voltage ripple and other quantities. Table 1 summarize the values that can be used for calculation.

After calculation, we opt to choose elements whose specifications are shown in the following table 2.

3.2 Design of the control part of the converter

3.2.1. Modulation technique

To control the switches, there are many techniques. In our case basing on the study of these papers [35]–[37], we chose the unipolar PWM technique.

In this technique, we use a carrier signal V_C that has a triangular form defined by an amplitude $V_{C_{MAX}}$ and a frequency f_C. We use also, two modulating signals (V_M and $-V_M$) that have a sinusoidal form and have the same amplitude $V_{M_{MAX}}$ and the same frequency f_M. Furthermore, the two modulating signals are shifted by π. Because there are a π phase shift the even harmonics in the output voltage will be eliminated.

Table 1: Values of different electrical quantities used for the calculation.

Quantity		Unit	Value
DC link voltage VDC	Min	Volt (V)	249
	Max	Volt (V)	358
Maximum voltage ripple ΔV_{DC}		Volt (V)	49
Input voltage frequency		Hertz (Hz)	50
AC output voltage *Vo*		Volt (V)	120
AC output current *Io*		Ampere (A)	5
Power Factor cos φ		-	0.5

Table 2: Specifications of converter elements

Diodes bridge	Capacitor filter		Switches	LC Filter		AC Load	
	C+	*C-*		*Lf*	*Cf*	*Ro*	*Lo*
If = 2A V_{RRM} *= 200V*	*470µF, 200V*	*470µF, 200V*	*IGBT 40A, 600V*	*32mH*	*127µF, 200V*	*12Ω*	*66mH*

An inverter that use this modulation technique has, at the output, a fundamental component amplitude defined by this formula

$$V'_{o1_{MAX}} = m_a \, . V_{DC} \tag{5}$$

Where m_a is the modulation index, it presents the amplitude ratio of the carrier signal and the modulating signal. It is defined by this formula:

$$m_a = \frac{V_{M_{MAX}}}{V_{C_{MAX}}} \tag{6}$$

To generate the PWM signal we compare the carrier signal with the two modulating signals and we have:

For the Q1, Q4 branch:

- When $V_M > V_C$, the switch Q1 is ON and the switch Q4 is OFF
- When $V_M < V_C$, the switch Q1 is OFF and the switch Q4 is ON

For the Q2, Q3 branch:

- When $-V_M > V_C$, the switch Q2 is ON and the switch Q3 is OFF
- When $-V_M < V_C$, the switch Q2 is OFF and the switch Q3 is ON

Figure 6 presents the PWM signals generated by this technique, as well as, table 3 presents the switches states and different values of the VSI output. We note that the VSI output can have three levels: $-V_{DC}$, *0* and $+V_{DC}$.

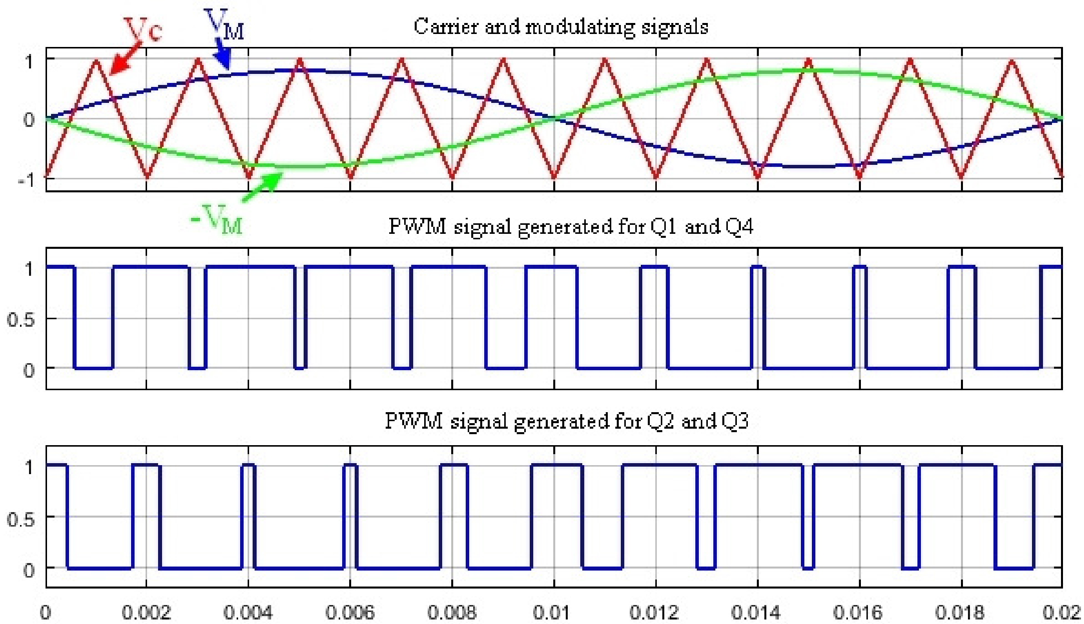

Figure 6: Carrier and modulating signals forms and PWM signals generated with a carrier frequency equals 500Hz and a modulation index equals 0.8.

Table 3: Switches states and VSI output values.

State N	$Q1\&\overline{Q4}$	$Q2\&\overline{Q3}$	V_{AN}	V_{BN}	V_{AB}
1	ON	ON	$V_{DC}/2$	$V_{DC}/2$	0
2	OFF	OFF	$-V_{DC}/2$	$-V_{DC}/2$	0
3	ON	OFF	$V_{DC}/2$	$-V_{DC}/2$	V_{DC}
4	OFF	ON	$-V_{DC}/2$	$V_{DC}/2$	$-V_{DC}$

3.2.2. Control technique

The converter must compensate the increasing or decreasing of the voltage, and it should compensate the voltage ripple due to the charging and discharging of the capacitors. Because, referring to formula 5, if the input voltage varies, the DC voltage varies, then the output voltage varies.

As the variations are only at the input of the inverter, furthermore, we use a known linear load. We designed a control based on a feedforward technique. In this technique, we sense the input variations and we adjust the PWM signals, in such a way to have at the output of the converter a stable voltage.

For example in Morocco, the voltage can vary between 249V and 358V, and taken in consideration the voltage ripple it can decrease to 200V. We can rewrite the formula 5 as follows:

$$V'_{o1_{MAX}} = m_a \,.(V_{DC_{REF}} \pm V_{DC_{VAR}}) \tag{7}$$

Where $V_{DC_{REF}}$ is a chosen DC voltage reference, and $V_{DC_{VAR}}$ is the variations around the DC voltage reference. We chose a DC voltage reference equals 311V, which corresponds to

$220V_{RMS}$. This value is the nominal value provided by the electrical operator in Morocco [27].

Now we see that $V'_{o1_{MAX}}$ is influenced by the voltage variations. To eliminate these variations, we must adjust either $V_{M_{MAX}}$ or $V_{C_{MAX}}$. If we choose $V_{M_{MAX}}$ we must calculate at each time its value by this formula:

$$V_{M_{MAX}} = V_{M_{REF}} \times \frac{V_{DC_{REF}}}{(V_{DC_{REF}} \pm V_{DC_{VAR}})} \tag{8}$$

Where $V_{M_{REF}}$ is a reference value calculated by the formula 5, by replacing V_{DC} by $V_{DC_{REF}}$ value and replacing $V'_{o1_{MAX}}$ by the desired value.

Figure 7 present the adjustment of the modulation index according to the voltage error (voltage variations).

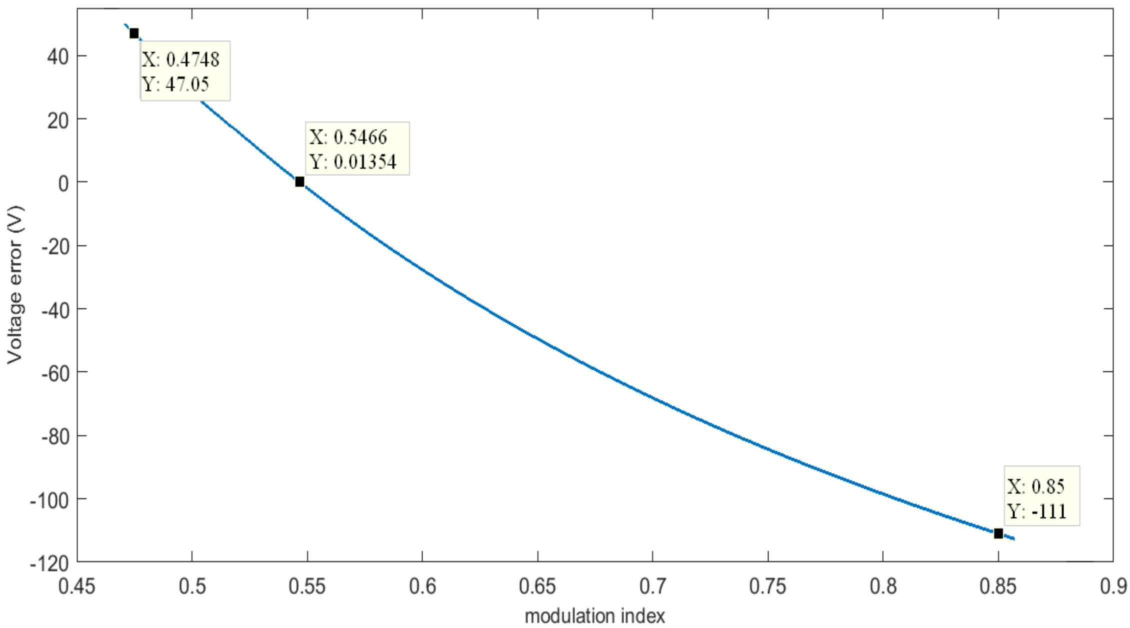

Figure 7: Voltage error vs modulation index.

Finally, if we put the result of formula 8 in formula 7 of $V'_{o1_{MAX}}$ voltage, we find:

$$V'_{o_{MAX}} = \frac{V_{M_{REF}}}{V_{C_{MAX}}} V_{DC_{REF}} \qquad \forall\, V_{DC_{VAR}} \tag{9}$$

As we see, by applying this technique, the amplitude of the output voltage of the converter remains stable regardless of the input voltage variation.

3.2.3. Control program

To generate the PWM signals we opted to use a digital controller. The control technique is implemented as a program into a microcontroller in discrete form. The frequency of carrier signal chosen is *1 kHz*. We used a sampling step equals 50µs that corresponds to a sample frequency equals *20 kHz*. We note that the Nyquist-Shannon theorem is respected.

The program implemented in the microcontroller is presented by the flow charts at figure 8. The flow chart (a) presents the main function. This function is responsible for the initialization of the microcontroller, the reading of the V_{DC} value from the register which records the result of the conversion of the ADC, and the adjustment of the $V_{M_{MAX}}$ value. The flow chart (b) presents the interrupt function. An interruption is generated each 50us. Into this function after the interrupt call, we compare the value of the carrier signal with the values of the modulating signals, taken in consideration the adjustment. In the comparison, we take the samples that correspond to the same time. We note that as the microcontroller turns at a high frequency (*48MHz*) the comparison between V_C and V_M and between V_C and -V_M is performed almost at the same time.

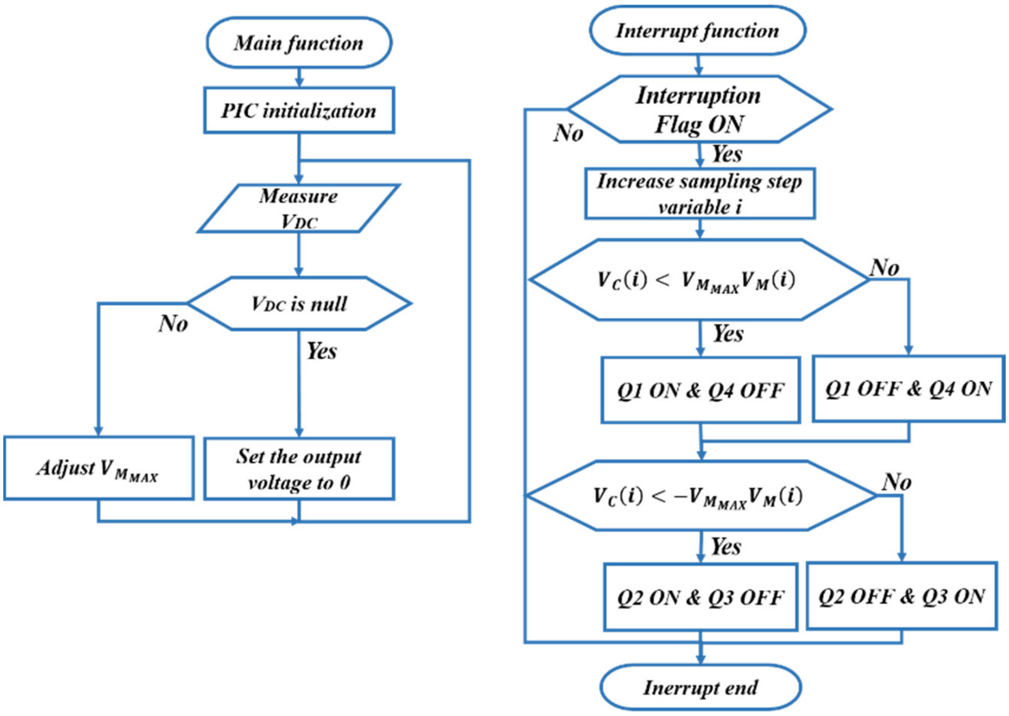

(a) (b)

Figure 8: Flow charts of the program implemented in the microcontroller: (a) Main function, (b) Interrupt function.

4. Simulation results and experimental results

4.1. Results of simulations and tests of digital control

The program presented in the past section, is implemented in a microcontroller PIC18F2550. We will present some results from elaborated tests. In figure 9(a) we see the PWM signals generated by the microcontroller with a carrier frequency equals 500Hz and an modulation index equals 0.8. If we compare them with the signals generated by a simulation in MATLAB (figure 9(b)), we can see that are practically the same.

In figure 10 we present another comparison between a PWM signals generated by the microcontroller (figure 10(a)) and PWM signals generated on MATLAB (figure 10(b)). In this test we use a carrier frequency equals *1 kHz* and a modulation index equals 0.8.

To validate the control program, we tested the algorithm with a variable input, and we had results that are presented in figure 11. We have chosen a low carrier frequency (*250Hz*) in order to be able to view the changes. Figure 11(a) present the results when the input voltage equals 200V and that corresponds to a modulation index equals 0.85. Figure 11(b) present the results when the input voltage increase to 358V that corresponds to a modulation index equals 0.475. We notice that the pulse width changes by changing the input voltage. When the input voltage decrease the pulse width increase and vice versa.

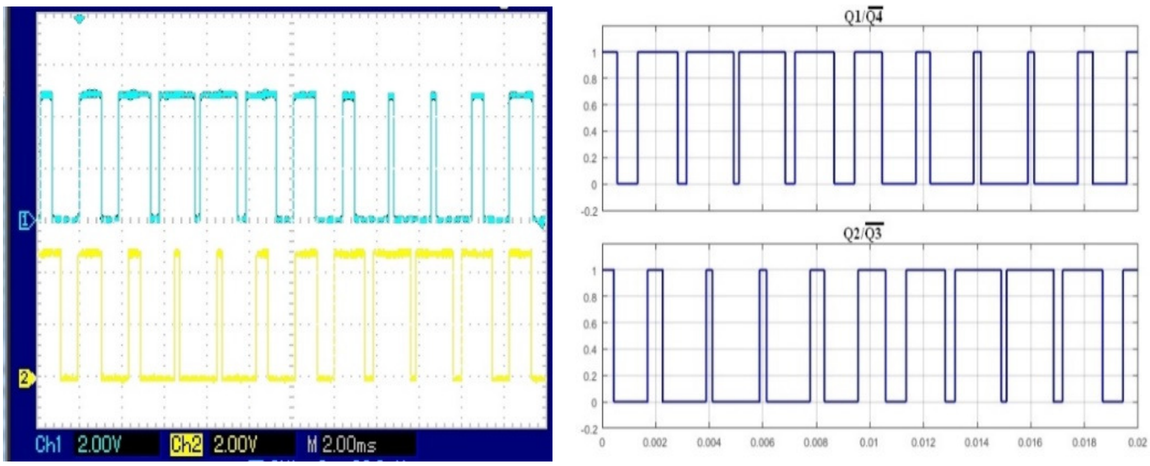

(a) (b)

Figure 9: (a) PWM signals generated by the microcontroller. (b) PWM signals generated by MATLAB.

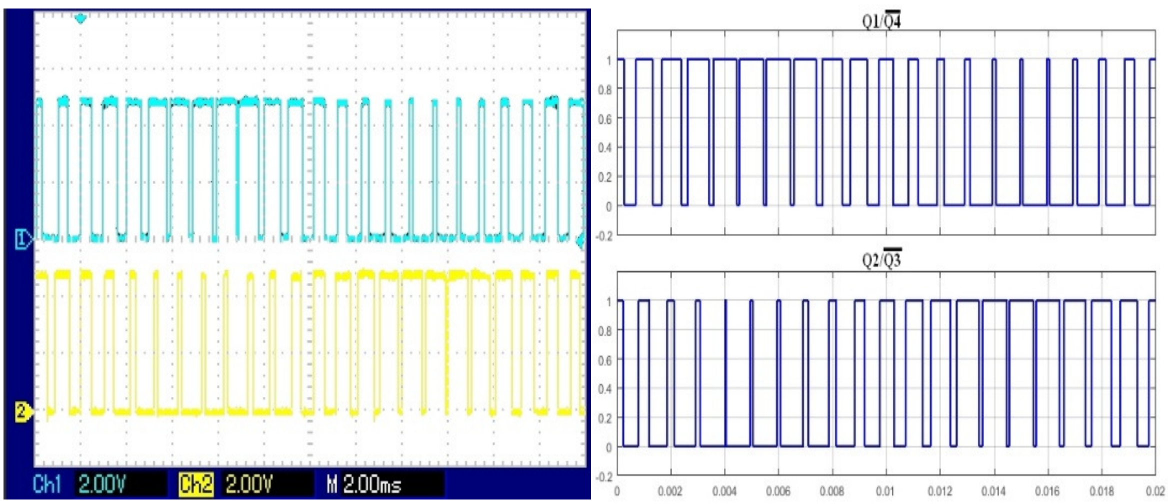

(a) (b)

Figure 10: (a) PWM signals generated by the microcontroller. (b) PWM signals generated by MATLAB.

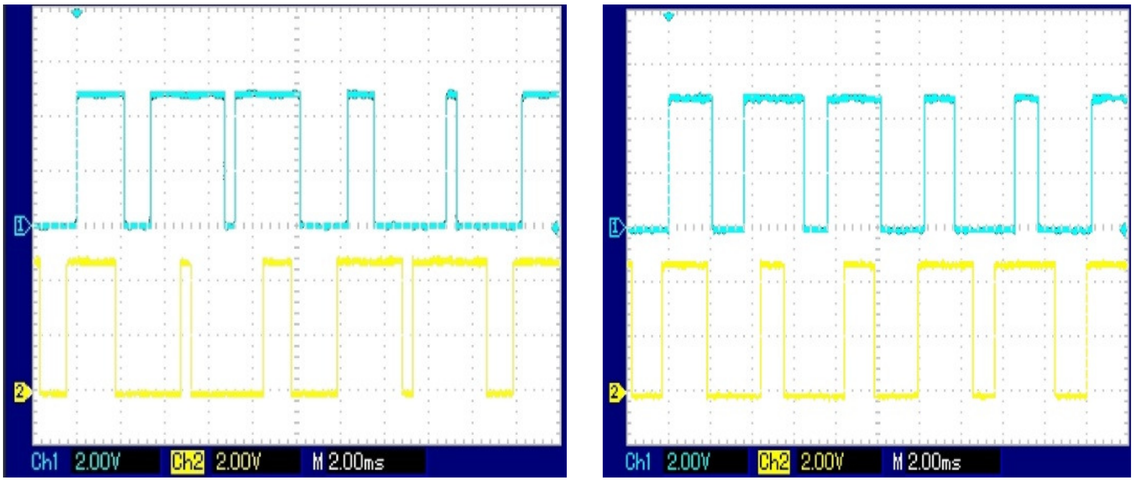

(a) (b)

Figure 11: PWM signals generated by the microcontroller. (a) Input voltage equals 200V. (b) Input voltage equals 358V.

4.2. Results of simulations of AC-AC converter circuit

The circuit presented in figure 4 is realized in MATLAB Simulink. All blocks mentioned before (rectifier, inverter...) are chosen as the performed study. We have used as AC input voltage a modified source. This source provides a voltage whose the amplitude varies during the time. The amplitude increase from 249V to 358V.

As results, we present firstly the output voltage of the VSI. Figure 12 present the output voltage waveform without filter or load. We notice that in this figure the amplitude of the output voltage increases and follows the amplitude of the input voltage. But, if we look at figures 13(b), 14(b) and 15(b), that present respectively the portions (A), (B) and (C) we notice that the pulse width changes, it decreases by the increasing of the input voltage. Furthermore, if we refer to figures 13(a), 14(a) and 15(a) where they present the spectrums of the output voltage when the amplitude of input voltage is at 249V, 311V and 358V respectively. We deduce that the amplitude of the fundamental component remains practically stable.

As second results, when we added the LC filter and the AC load. We notice that the AC output voltage of the AC-AC converter is a good sinusoidal waveform (figure 16). This is justified by the low THD (figure 17(b)). Furthermore, the voltage amplitude remains stable (equals 120V RMS) even if the amplitude of the AC input voltage changes.

For the current, we obtained a good sinusoidal waveform (figure 16), as well as the amplitude equals 7A that corresponds to a RMS value equals 5A.

As last result of the simulation. The phase shift between the current and the voltage equals 3.33ms that corresponds to a 60° phase shift.

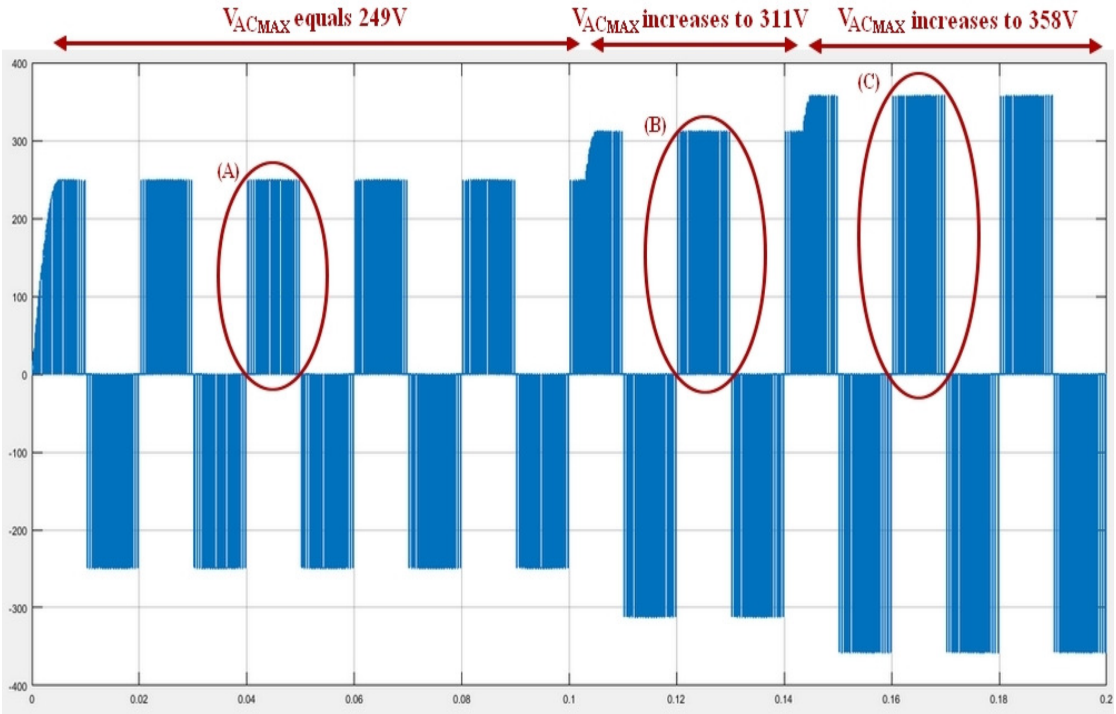

Figure 12: Output voltage waveform of the converter without filter or load.

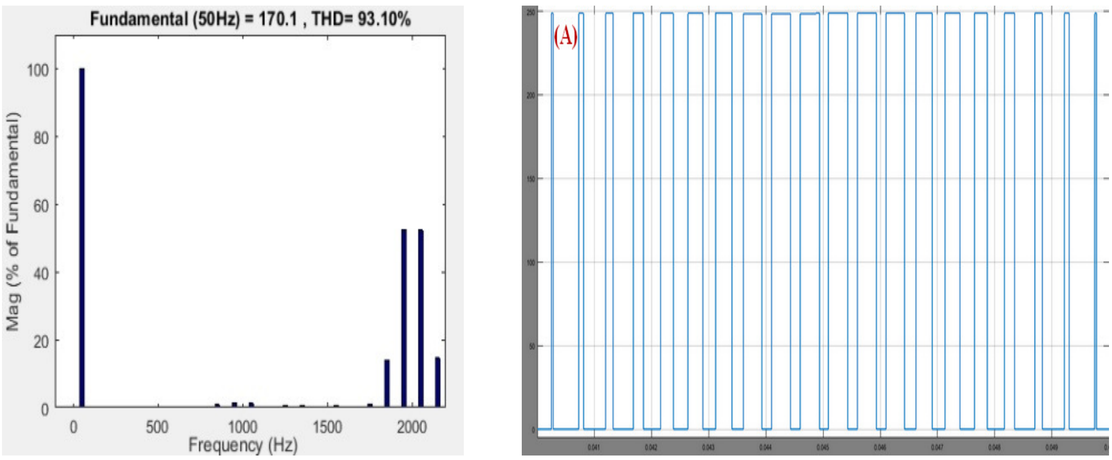

(a) (b)

Figure 13: Output voltage of the converter when the amplitude of input voltage is at 249V. (a) Spectrum. (b) Part (A) of figure 12.

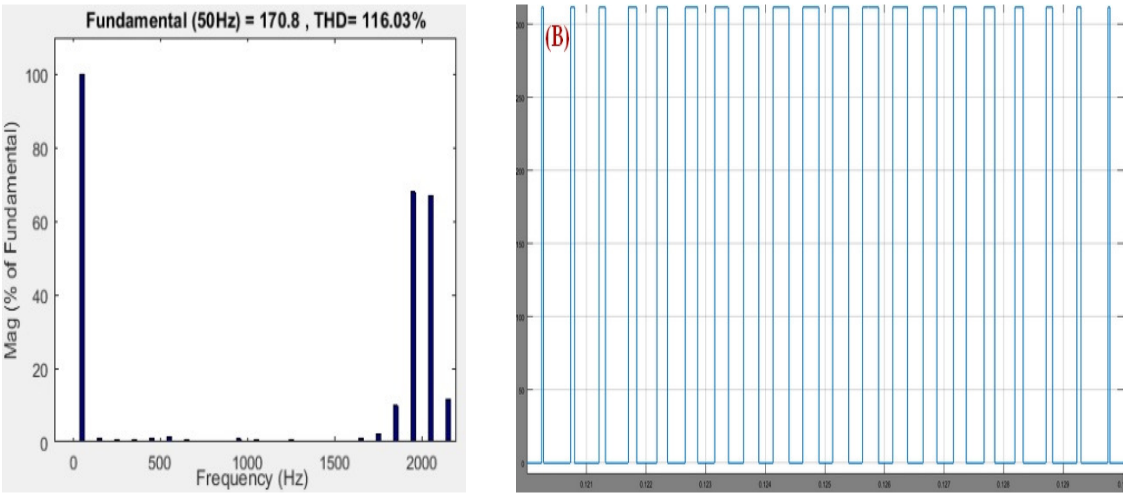

(a) (b)

Figure 14: (a) Output voltage of the converter when the amplitude of input voltage is at 311V. (a) Spectrum. (b) Part (B) of figure 12.

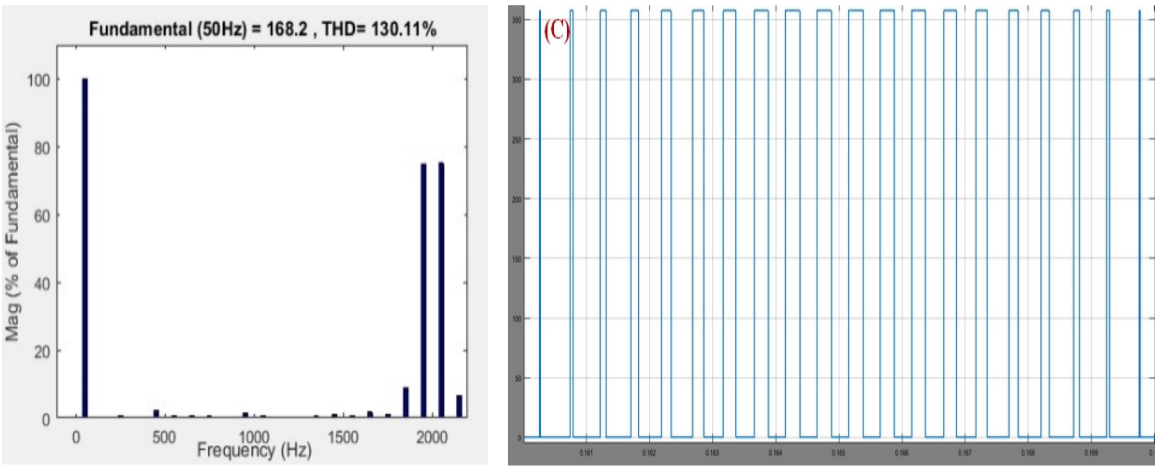

(a) (b)

Figure 15: Output voltage of the converter when the amplitude of input voltage is at 358V. (a) Spectrum. (b) Part (C) of the figure 12.

5. Conclusion

Today's electrical grid requires serious improvements in control, diagnostics and energy management. Electricity operators need a real-time monitoring of the network state as well as the measurement equipment state. For this reason, researchers are trying to design measurement instruments that are completely accessible remotely in order to read the consumption information and the state of the measuring instrument itself. Moreover the control and the execution of the tasks remotely if it was necessary, like the precision test of the electric meters. Through this paper, our contribution in this area of research is to automate the calibration process. Indeed, energy measurement systems need to be calibrated, in such a way to eliminate the measurement errors. The calibration process was performed at laboratory, but currently, we need to perform this process on site and periodically. For this reason, during our study of the structure of the smart meter, we have the idea to integrate a calibration card into the energy measurement, to perform the calibration on site and remotely, and to be able to manage many meters (check their accuracy) in a short time.

To be able to perform the accuracy test or to calibrate the meter, we need a stable power source used as reference. We cannot use the power line because, for this power source, the voltage can vary, and we cannot know at the moment of the calibration how much is the voltage value. For that, we designed an AC-AC converter included in the calibration card. The role of this converter is to provide a stable known AC voltage at the output, even if the voltage line that can vary supplies it. Moreover, the current is fixed by a known AC load.

The designed converter is an indirect AC-DC-AC converter. In such structure, we convert the AC voltage to a DC voltage, then, we use a voltage source inverter to generate the AC output voltage. The rectifier is a simple diode bridge and a filter capacitor, as well as, the voltage source inverter has an H-bridge single-phase structure. As has been mentioned, the choose of this structure is to minimize the components. We note that to stabilize the AC output voltage we used a feedforward technique. In this technique, and because the AC input voltage which varies, we correct the modulation index, by calculating the AC input error, this by comparing the instantaneous DC voltage value with a DC voltage reference.

To validate our design, we simulated the whole circuit on MATLAB Simulink. The results, presented before, prove that we reached our objective, which is to provide a stable power source at the output of the AC-AC converter, even if the AC input voltage varies. Furthermore, the control technique has been tested experimentally, and we noticed that the PWM signals change according to the input error.

As results, the AC output voltage remains stable at 120V even if the AC input voltage varies. The AC output current is stable and equals 5A. It is fixed by the AC load. The AC voltage and the AC current are used to correct the gain values of the voltage chain and the current chain respectively. There is a 60° phase shift between the current and the voltage that is used to compensate the phase shift error added by the measurement system.

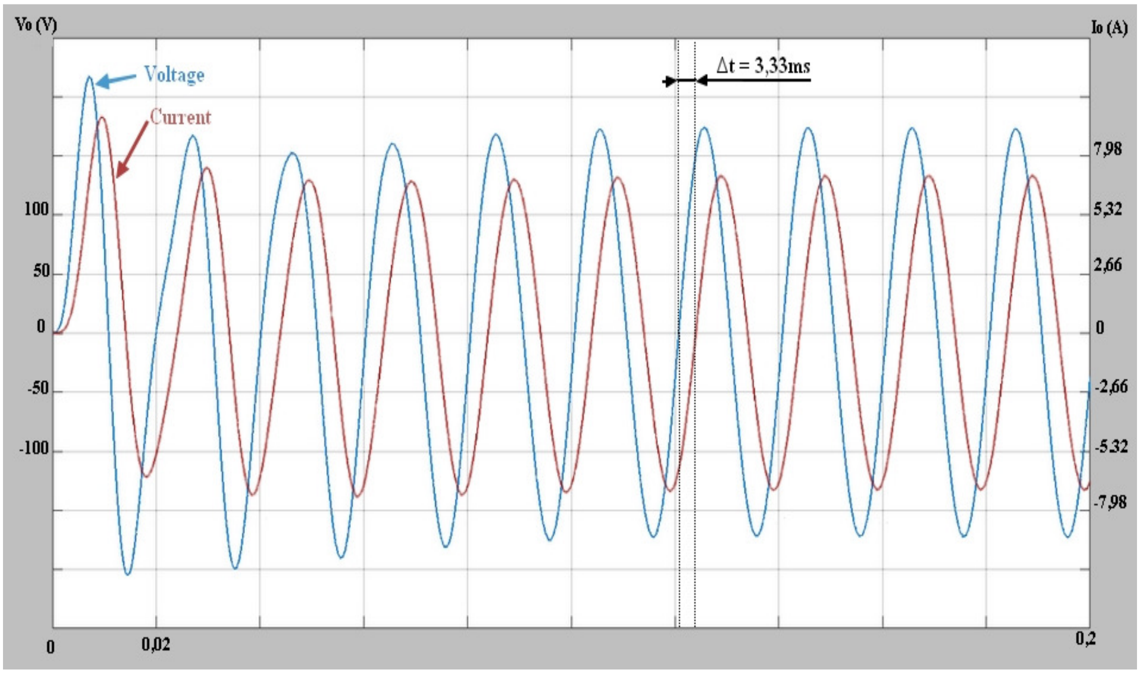

Figure 16: output voltage and current waveforms of the Converter with filter and load.

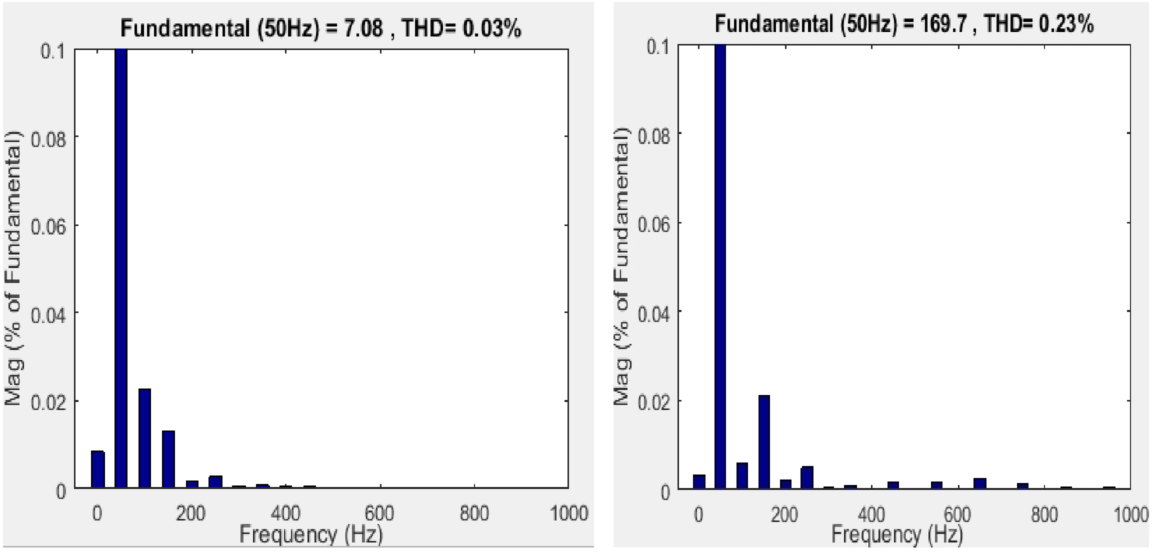

(a) (b)

Figure 17: (a) Spectrum of the output current of the converter. (b) Spectrum of the output voltage of the converter.

References

[1] R. S. Pukale, S. V Bavache, S. N. Kashid, A. P. Sabale, P. P. Patil, and P. H. Shinde, "Automatic meter reading of electricity by using power line communication," in *2017 International Conference on Innovations in Green Energy and Healthcare Technologies (IGEHT)*, 2017, pp. 1–5.

[2] G. Wu *et al.*, "Design and implement of baseband circuits for a wireless automatic meter reading application," in *2016 IEEE International Conference on Electron Devices and Solid-State Circuits (EDSSC)*, 2016, pp. 395–398.

[3] D. Xuzhi, L. Zhijuan, Z. Jin, and H. Lu, "The development and operation of integrated automatic meter reading system in Shanghai," in *2016 IEEE PES Asia-Pacific Power and Energy Engineering Conference (APPEEC)*, 2016, pp. 1675–1678.

[4] G. Yao, H. Zhang, and Q. Chen, "A wireless automatic meter reading system based on digital image process and ZigBee-3G," in *2014 IEEE International Conference on System Science and Engineering (ICSSE)*, 2014, pp. 128–132.

[5] J. Matanza, S. Alexandres, and C. Rodriguez-Morcillo, "Automatic Meter-Reading Simulation through Power Line Communication," in *2013 IEEE 21st International Symposium on Modelling, Analysis and Simulation of Computer and Telecommunication Systems*, 2013, pp. 283–287.

[6] K. Ashna and S. N. George, "GSM based automatic energy meter reading system with instant billing," in *2013 International Mutli-Conference on Automation, Computing, Communication, Control and Compressed Sensing (iMac4s)*, 2013, pp. 65–72.

[7] R. Morello, C. De Capua, G. Fulco, and S. C. Mukhopadhyay, "A Smart Power Meter to Monitor Energy Flow in Smart Grids: The Role of Advanced Sensing and IoT in the Electric Grid of the Future," *IEEE Sens. J.*, vol. PP, no. 99, p. 1, 2017.

[8] R. Morello, S. C. Mukhopadhyay, Z. Liu, D. Slomovitz, and S. R. Samantaray, "Advances on Sensing Technologies for Smart Cities and Power Grids: A Review," *IEEE Sens. J.*, vol. PP, no. 99, p. 1, 2017.

[9] S. Chatterjee, V. Archana, K. Suresh, R. Saha, R. Gupta, and F. Doshi, "Detection of non-technical losses using advanced metering infrastructure and deep recurrent neural networks," in *2017 IEEE International Conference on Environment and Electrical Engineering and 2017 IEEE Industrial and Commercial Power Systems Europe (EEEIC / I CPS Europe)*, 2017, pp. 1–6.

[10] V. Paciello, A. Pietrosanto, and P. Sommella, "Smart Sensors for Demand Response," *IEEE Sens. J.*, vol. PP, no. 99, p. 1, 2017.

[11] M. Manbachi and M. Ordonez, "AMI-based Energy Management for Islanded AC/DC Microgrids Utilizing Energy Conservation and Optimization," *IEEE Trans. Smart Grid*, vol. PP, no. 99, p. 1, 2017.

[12] E. J. Palacios-Garcia *et al.*, "Using smart meters data for energy management operations and power quality monitoring in a microgrid," in *2017 IEEE 26th International Symposium on Industrial Electronics (ISIE)*, 2017, pp. 1725–1731.

[13] G. Zhang, T. Tan, and G. Wang, "Real-Time Smart Charging of Electric Vehicles for Demand Charge Reduction at Non-Residential Sites," *IEEE Trans. Smart Grid*, vol. PP, no. 99, p. 1, 2017.

[14] V. Monteiro, J. C. Ferreira, J. G. Pinto, and J. L. Afonso, "New Opportunities and Perspectives for the Electric Vehicle Operation in Smart Grids and Smart Homes Scenarios," in *e 3rd International Conference on Vehicle Technology and Intelligent Transport Systems (VEHITS 2017*, 2017, no. Vehits, pp. 400–407.

[15] J. A. Afonso, F. Rodrigues, P. Pereira, H. Gonçalves, and J. L. Afonso, "Wireless Monitoring and Management of Energy Consumption and Power Quality Events," in *World Congress on Engineering 2015*, 2015, vol. I.

[16] A. Bernieri, L. Ferrigno, M. Laracca, and C. Luongo, "A Discussion about the Effect of the MID Directive on the Calibration of Electrical Energy Meters," in *2008 43rd International Universities Power Engineering Conference*, 2008, no. ii, pp. 1–5.

[17] G. Aurilio, D. Gallo, C. Landi, and M. Luiso, "AC Electronic Load for On-Site Calibration of Energy Meters," in *2013 IEEE International Instrumentation and Measurement Technology Conference (I2MTC)*, 2013, pp. 768–773.

[18] A. D. Femine, D. Gallo, C. Landi, and M. Luiso, "Advanced instrument for field calibration of electrical energy meters," *IEEE Trans. Instrum. Meas.*, vol. 58, no. 3, pp. 618–625, 2009.

[19] A. D. Femine, S. Member, D. Gallo, C. Landi, and M. Luiso, "Measurement Equipment for On-Site Calibration of Energy Meters," *Power Qual.*, pp. 1–6, 2007.

[20] L. Guoying and C. Yinglin, "Research for Calibration Technology of Digital Input Electric Energy Meter," in *CICED 2010 Proceedings*, 2010, pp. 1–6.

[21] T. Hou and Y. H. Guo, "Research of Calibration Instrument of Multi-Site Single-Phase Energy Meter," *Appl. Mech. Mater.*, vol. 273, pp. 424–427, 2013.

[22] J. Z. R. Arseneau, M. Frigault, "IMPROVING THE ACCURACY OF THE ON-SITE CALIBRATIONS OF MULTI-FUNCTION ELECTRICAL STANDARDS," in *2008 Conference on Precision Electromagnetic Measurements Digest*, 2008, pp. 84–85.

[23] D. Amicone, A. Bernieri, L. Ferrigno, and M. Laracca, "A smart add-on device for the remote calibration of electrical energy meters," *2009 IEEE Intrumentation Meas. Technol. Conf. I2MTC 2009*, no. May, pp. 1599–1604, 2009.

[24] Z. Jebroni, H. Chadli, B. Tidhaf, A. Benlghazi, and A. Tahani, "Gain Correction and Phase Compensation of a Smart Electrical Energy Meter," in *2016 International Conference on Engineering & MIS (ICEMIS)*, 2016, no. 1, pp. 1–6.

[25] Z. Jebroni, H. Chadli, B. Tidhaf, and E. Chadli, "Design of a calibration board integrated in a smart electrical energy meter (hardware part)," in *2017 International Conference on Wireless Technologies, Embedded and Intelligent Systems (WITS)*, 2017, no. 1.

[26] ONEE-BE, "Activity report," 2015.

[27] ONEE-BE, "Specification technique: Compteurs numériques d'énergie électrique évolutif Pour clients basse tension," no. 212. 2014.

[28] F. Clarizia, D. Gallo, C. Landi, M. Luiso, and R. Rinaldi, "Smart Meter Systems for Smart Grid management," in *Instrumentation and Measurement Technology Conference Proceedings (I2MTC), 2016 IEEE International*, 2016.

[29] Ž. Nakutis, M. Saunoris, and V. Daunoras, "A Method for Remote Wattmeter Calibration," in *Instrumentation and Measurement Technology Conference (I2MTC), 2017 IEEE International*, 2017.

[30] Cirrus, "Two Channel Energy Measurement IC," vol. 2013. 2013.

[31] H. Kim and S. Sul, "A Novel Filter Design for Output LC Filters of PWM Inverters," vol. 11, no. 1, pp. 74–81, 2011.

[32] J. K. Steinke, "Use of an LC filter to achieve a motor-friendly performance of the PWM voltage source inverter," *IEEE Trans. Energy Convers.*, vol. 14, no. 3, pp. 649–654, 1999.

[33] Khaled H.Ahmed, "Passive filter design for three phase inverter interfacing in distributed generation," *Electr. power Qual. uitilisation*, 2007.

[34] J. Kim, J. Choi, and H. Hong, "Output LC filter design of voltage source inverter considering the\nperformance of controller," *PowerCon 2000. 2000 Int. Conf. Power Syst. Technol. Proc. (Cat. No.00EX409)*, vol. 3, pp. 1659–1664, 2000.

[35] B. A. Hamidah and M. Tohtayong, "Selective Harmonics Elimination Technique," in *2016 IEEE Student Conference on Research and Development (SCOReD)*, 2016, pp. 11–14.

[36] S. Maheshri and P. Khampariya, "Simulation of single phase SPWM (Unipolar) inverter," vol. 1, no. 9, pp. 12–18, 2014.

[37] A. Namboodiri and H. Wani, "Unipolar and Bipolar PWM Inverter," *IJIRSRT - Int. J. Innov. Res. Sci. Technol.*, vol. 1, no. 7, p. 7, 2014.